

Modeling proton mobility in acidic zeolite clusters. I. Convergence of transition state parameters from quantum chemistry

Justin T. Fermann and Cristian Blanco

Department of Chemistry, University of Massachusetts, Amherst, Massachusetts 01003

Scott Auerbach^{a)}

Department of Chemistry, and Department of Chemical Engineering, University of Massachusetts, Amherst, Massachusetts 01003

(Received 30 August 1999; accepted 24 January 2000)

We have applied electronic structure methods to the calculation of transition state parameters for the O(1)→O(4) proton transfer in H-Y zeolite. We arrive at a set of recommendations for calculating these transition state parameters accurately and efficiently. Density functional theory using the B3LYP functional and basis sets of triple- ζ quality in the valence space, and including polarization functions on all atoms, is the most efficient method for converging structures and vibrational frequencies. For converging classical barrier heights, we find it necessary to augment MP2 barrier heights calculated using large basis sets with MP4 energies obtained in more limited basis sets. We obtain an O(1)→O(4) barrier height of 86.1 kJ mol⁻¹, and find the curvature of the barrier at the transition state to be 1570 cm⁻¹. Including long range effects from the work of Sauer *et al.* [ACS Symp. Ser. **721**, 358 (1999)] results in a higher barrier, which we estimate to be 97.1 kJ mol⁻¹. We attribute the fact that our barriers are significantly larger than those reported in the experimental literature to the neglect of tunneling in the interpretation of experimental data. © 2000 American Institute of Physics. [S0021-9606(00)70815-4]

I. INTRODUCTION

Zeolites are used as shape-selective catalysts in a variety of important petrochemical processes such as cracking and reforming.^{1,2} The activity of zeolite catalysts is often associated with Brønsted acid sites, which have the form ≡Si-OH-Al≡. Understanding the microscopic dynamics of acidic protons in zeolites can shed light on how these catalysts function. The fact that zeolites such as H-Y and H-ZSM-5 are strong acids suggests that protons may be able to jump among oxygens in an AlO₄ tetrahedron, even in the absence of nucleophilic guests. Indeed, recent ¹H NMR measurements on acidic zeolites reveal significant proton mobilities with surprisingly low activation energies, depending on the zeolite and Si:Al ratio studied. For example, Baba *et al.* report activation energies of 19 and 28 kJ mol⁻¹ for H-ZSM-5³ and H-mordenite,⁴ respectively; while Sarv *et al.*⁵ report 45, 54, and 61 kJ mol⁻¹ for H-ZSM-5, H-mordenite, and H-Y, respectively. The broad disagreement among these experimental results suggests that we must first understand proton mobilities in bare zeolites before attempting to model zeolite catalysis in its full complexity. In this paper, denoted Paper I, we apply electronic structure methods to calculate transition state parameters for the O(1)→O(4) proton transfer in H-Y zeolite; while in the following paper, denoted Paper II, we develop and apply a novel harmonic semiclassical transition state theory to calculate quantum proton transfer rates.

Modeling zeolite acid sites with electronic structure

methods has received a great deal of attention in recent years.^{2,6-8} However, relatively few studies have been devoted to calculating transition state parameters for proton transfer processes,⁹⁻¹⁴ and even fewer studies have determined the extent to which these parameters are converged with respect to basis set, level of theory, and cluster size.¹⁵⁻¹⁷ Establishing such convergence is crucial for accurately modeling transition states, which often requires extended basis sets and sophisticated treatments of electron correlation. In this paper, we perform a variety of electronic structure calculations on very small clusters, containing 1 and 3 tetrahedral atoms (Al or Si), to establish acceptable error bounds on key transition state parameters by using successively larger basis sets and higher levels of theory. Our goal is to develop a set of recommendations for calculating these transition state parameters accurately and efficiently using the methods of quantum chemistry. Although in the present study we ignore long range forces, and hence cannot provide the most accurate model of H-Y,¹⁷ our study is valuable because the recommendations we make can be employed in future work using successively larger clusters, periodic models, or embedded cluster methods.

We find below that Hartree-Fock^{18,19} and BLYP^{20,21} density functional theory (DFT) calculations do not accurately describe this proton transfer process. DFT calculations using the B3LYP functional^{21,22} and basis sets of triple- ζ quality in the valence space, and including polarization functions on all atoms, provide the most efficient method for converging structures and vibrational frequencies. Unfortunately, this technique fails to predict the electronic energy at the relevant stationary points with sufficient accuracy. For converging

^{a)}Author to whom correspondence should be addressed. Electronic mail: auerbach@chem.umass.edu

classical barrier heights, we find it necessary to augment MP2²³ barrier heights calculated using large basis sets with MP4^{24,25} energies obtained in more limited basis sets. The barriers calculated below turn out to be significantly larger than those reported in the experimental literature.^{3–5} We attribute this discrepancy to the neglect of tunneling in the interpretation of experimental data (see Paper II).

The remainder of this paper is organized as follows: in Sec. II A we describe the molecular clusters used to model the active site, and in Sec. II B we outline the sequence of electronic structure methods used to approach convergence with respect to the basis set size and level of theory. In Sec. III we detail the results of our investigations organized by cluster type, compare our results with experimental data, and provide recommendations for future proton transfer calculations. In Sec. IV we give concluding remarks and foreshadow the major findings in Paper II.

II. METHODS

In this section we begin by presenting the molecular models used to study the proton transfer reaction between the O(1) and O(4) bridging oxygens in H–Y zeolite. This is followed by a description of the electronic structure methods used to parametrize the potential energy surface for proton hopping, as well as a discussion of our expectations regarding the accuracy of those methods.

A. Zeolitic cluster models

We have employed three molecular clusters to approximate the mobility of the acidic proton at a zeolite acid site. The simplest cluster, which was used primarily to investigate the convergence properties of the electronic structure calculations, consists of a single aluminum III coordinated to four OH[–] ligands. A proton added to this system effectively makes one of the OH[–] ligands into a water molecule, which can then donate its extra proton to another OH[–]. We refer to this as the 1T cluster, for the single tetrahedrally coordinated atom. This cluster is shown in Fig. 1 with geometrical parameters discussed in Sec. III A.

The second and third molecular cluster models both involve 3T clusters with H₃SiOAl(OH)₂OSiH₃[–] connectivity.^{6,9,17,26} The second cluster models a symmetric proton transfer reaction by constraining the 3T cluster to have a plane of symmetry along the SiOAlOSi backbone, and fixing the distance between the silicon atoms at two characteristic values: 5.8 Å and 6.0 Å.²⁷ The symmetry of these 3T clusters facilitates convergence studies for comparison with the 1T results. These clusters also provide model systems for exploring how proton transfer barriers vary with Si–Si distance. As expected, we find that the classical barrier height for proton transfer increases significantly with increasing Si–Si distance. For brevity, we do not discuss the results obtained using this cluster model in this paper, but they are of interest in determining dynamical trends and will be used in Paper II.

The third cluster mimics the O(1)→O(4) proton jump more accurately by extracting a cluster from H–Y neutron diffraction data.²⁸ We begin with the asymmetric unit of H–Y zeolite, extend it to three tetrahedral sites by including

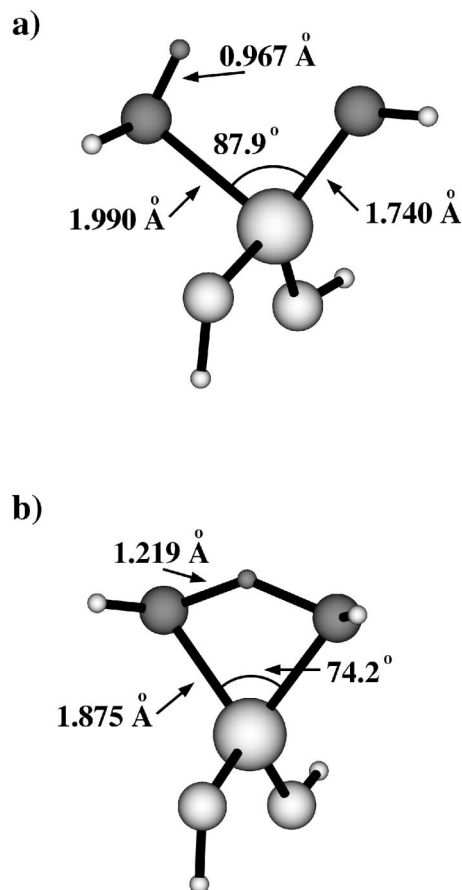


FIG. 1. Stationary points for the 1T cluster optimized at the MP2/6-311G(*d,p*) level of theory; (a) reactant (C_1 symmetry) and (b) transition state (C_s symmetry). Atoms participating in the proton transfer are darkened.

the two silicon atoms connected to the O(1) and O(4) bridging oxygens, and terminate the resulting cluster with hydrogen atoms. The terminal hydrogen atoms are placed in the directions of the next framework atoms, at distances of 1.4 Å for the fabricated SiH bonds and 0.9 Å for the fabricated OH bonds.²⁹ These hydrogen atoms are taken to represent the valency of the bulk zeolite from which our cluster model is extracted, and are kept frozen in space. All remaining atoms are allowed complete geometric freedom in the optimization process. This is equivalent to locking the terminal bonds of our cluster model to an infinitely massive cavity that has the same covalent footprint as a hole in H–Y zeolite, thereby including the mechanical restraints of the lattice. An illustration of this final cluster model is shown in Fig. 2, with geometrical parameters discussed in Sec. III B.

This final zeolite cluster yields our closest approximation to the proton transfer between the O(1) and O(4) bridging oxygens in H–Y zeolite. Sauer *et al.* have studied the effects of cluster size and embedding on the classical barrier height for this system using density functional theory (DFT).¹⁷ In what follows, we show that DFT underestimates classical barrier heights for these proton transfer systems, necessitating the use of explicitly correlated molecular orbital based methods, such as Møller-Plesset perturbation theory or coupled-cluster methods. In the future we will ap-

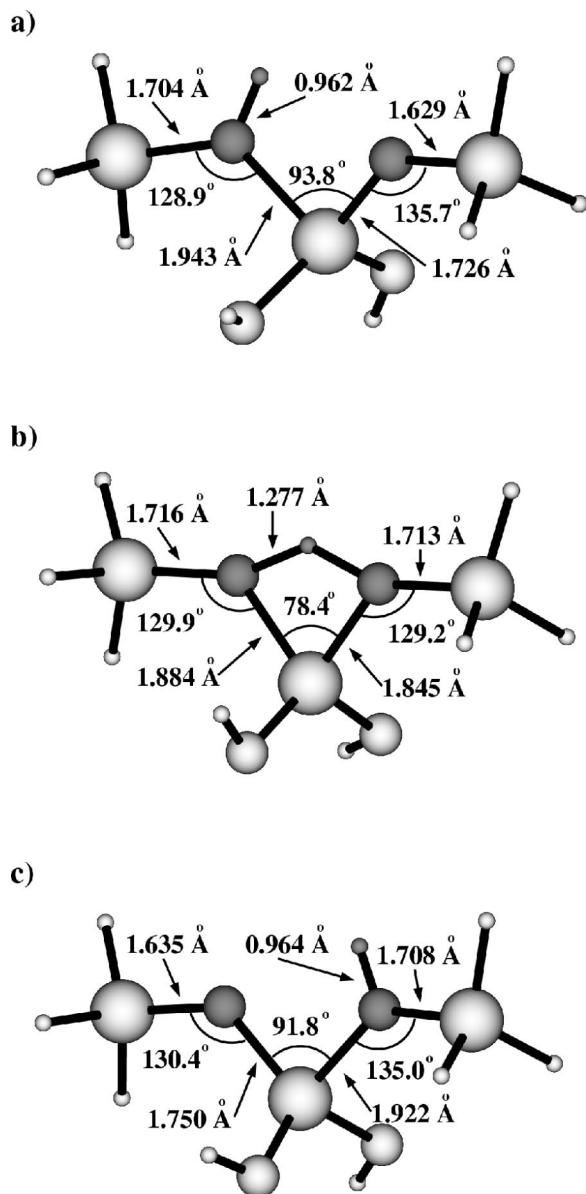


FIG. 2. Stationary points for the 3T cluster optimized at the MP2/6-311G(*d,p*) level of theory; (a) O(1) minimum, (b) transition state and (c) O(4) minimum. Atoms participating in the proton transfer are darkened.

ply these more sophisticated methods to larger clusters, embedded clusters, and periodic systems if possible, to quantify the effects of cluster size and long range forces on the electronic and vibrational characteristics of the system, since these play a crucial role in the proton jump process.

B. Electronic structure methods

Many previous studies have been reported exploring the structures and energetics of models of acidic zeolites.^{6,7} We show in the following paper that a reasonable estimate of the quantum rate coefficient is based on the zero point vibrational energy (ZPVE) corrected activation energy, ΔE_0 , and the curvature of the barrier at the transition state along the reaction coordinate q_F , $|\ddot{v}_F^\ddagger|$. In this paper we strive to de-

termine the optimal basis sets and levels of theory for calculating these particular rate theory parameters used to describe proton motion in zeolites.

A number of standard electronic structure methods were used to identify and vibrationally characterize the proton transfer events described above. For the 1T cluster, with equivalent reactants and products, the reactant and saddle point were identified with each theoretical methodology. The saddle point was found by symmetry restricted optimization of the cluster in the C_{2v} point group, which forces the proton to lie on the symmetric dividing surface. For the asymmetric cluster model based on infinitely massive terminal hydrogens, reactant and product minima and the transition state connecting them were located. In this case, the transition state was located by mode-following³⁰ in the proton transfer reaction coordinate. The nature of all critical points was verified by second derivative calculations and normal mode analysis *via* diagonalization of the mass weighted Hessian.

The basis sets we used included Pople split valence types^{31–38} and Dunning correlation consistent types^{39–43} accessible with the GAUSSIAN98 program set.⁴⁴ 6-31G and 6-311G core/valence Gaussian-type orbital (GTO) expansions were augmented incrementally with cartesian *d*-type polarization functions on heavy atoms [6-31G(*d*)], *p*-type polarization functions on hydrogens [6-311G(*d,p*)] and second sets of polarization functions on all atoms [6-311G(2*d*,2*p*)]. Correlation consistent polarized valence GTO basis sets with triple- ζ (cc-PVTZ) and quadruple- ζ (cc-PVQZ) expansions, which include polarization functions and are close to the complete basis set limit, were used for the 1T cluster to gauge the effects of basis set truncation at the 6-311G(*d,p*) level for the 3T cluster.

Electronic wave functions were obtained using Hartree-Fock (HF) theory,^{18,19} and dynamic correlation effects¹⁹ were incorporated using Møller-Plesset perturbation theory through second²³ (MP2) and fourth^{24,25} (MP4) order. Coupled-cluster methods including single and double excitations (CCSD)^{45,46} and a perturbative treatment of triple excitations [CCSD(T)]^{47,48} represent our most extensive treatment of electron correlation. We also utilized gradient corrected density functional theory (DFT) combining either the 1988 Becke exchange functional²⁰ with the Lee, Yang, and Parr correlation functional²¹ (BLYP) or the 1993 Becke 3-parameter exchange functional²² with the Lee, Yang, and Parr correlation functional (B3LYP) evaluated on high accuracy numerical integration grids. Other researchers¹² have reported success using the Becke Half-and-Half functional⁴⁹ as implemented in the GAUSSIAN98 suite;⁴⁴ we have avoided this functional due to ambiguities in its interpretation.⁵⁰

At all levels of theory except MP4, CCSD, and CCSD(T), analytic gradient techniques^{30,51,52} were used to locate the minimum energy structures and transition states along the proton transfer reaction pathway within the geometrical restraints mentioned above. At the optimized stationary points, unrestricted Cartesian coordinate gradients had magnitudes less than 10^{-5} h Bohr⁻¹. Analytic and numerical difference energy second derivative methods^{51,53,54} were used to evaluate harmonic vibrational frequencies, and to verify the stationary points found as corresponding to

minima and maxima along the reaction coordinate. In performing the normal mode analysis from energy second derivatives, we set the mass of the frozen hydrogens to a very large number (e.g., 10^6 a.u.);⁵⁵ this results in vibrational frequencies very similar to those observed for lattice modes in bulk Na-Y.⁵⁶ Due to the geometrical constraints imposed on the 3T cluster, the stationary points are not strictly minima or first order saddle points, because there exist up to five residual imaginary frequencies ($|\bar{\nu}| < 200 \text{ cm}^{-1}$) arising from constrained modes. In the 3T cluster, these imaginary modes map onto distortions of the bulk zeolite, and have frequencies of zero when the terminal hydrogens are made very massive and the Hessian matrix reanalyzed.

All calculations were performed using either the GAUSSIAN98⁴⁴ or PSI⁵⁷ suite of quantum chemistry programs. These programs were run on IBM RS/6000 AIX workstations, a four node IBM SP2 AIX computer, and Intel Linux workstations. Representative times for some of the larger calculations performed on the 3T cluster, indexed to a 333 MHz 604e Power PC RS/6000, are as follows: B3LYP/6-31G(*d*) frequencies, 10 CPU hours; MP2/6-311G(*d*) frequencies, 19 CPU hours; B3LYP/6-311G(*d,p*) frequencies, 23 CPU hours; and MP4/6-311G(*d,p*) energy, 48 CPU hours. The largest calculation reported here required approximately 5 gigabytes of disk space.

III. RESULTS AND DISCUSSION

A. 1T cluster

Figure 1 shows the structure of the energy minimum and transition state calculated for the proton transfer reaction in the 1T cluster, including the values of several important geometrical parameters at the highest level of theory at which optimizations were performed, MP2/6-311G(*d,p*). These values compare quite favorably with measured bond distances and angles from typical zeolite acid sites, but this cluster is too small to make such comparisons meaningful. The real importance of these results is in developing the minimum level of theory necessary to produce substantially converged geometries. We find that the bond lengths and angles shown cease to vary with respect to a basis set by more than 0.01 Å or 1°, respectively, once a 6-311G(*d,p*) description of the atomic orbitals in the molecule is used. B3LYP and MP2, both correlated levels of theory, give essentially identical geometrical results to within 0.01 Å or 1° for all germane parameters.

Table I shows the classical barrier height $\Delta V_0 = V_0^\ddagger - V_0^r$, the zero point vibrational energy (ZPVE) correction $\Delta \text{ZPVE} = \sum_{i=1}^{F-1} \hbar \omega_i^\ddagger / 2 - \sum_{i=1}^F \hbar \omega_i^r / 2$, the ZPVE corrected classical barrier height $\Delta E_0 = \Delta V_0 + \Delta \text{ZPVE}$, and the magnitude of the imaginary harmonic vibrational frequency at the transition state $|\bar{\nu}_F^\ddagger|$ of the 1T cluster. In what follows, a dash indicates a basis set/level of theory combination that is either deemed unnecessary or is beyond the scope of our computing resources. It is clear from our data that at the HF and B3LYP levels of theory, the 6-311G(*d,p*) basis set is adequate for modeling the proton transfer reaction, and that very little is to be gained from the added expense of more

TABLE I. Summary of electronic structure results for 1T cluster. Energies in kJ mol^{-1} .

Level of theory	Basis set [NBF ^a]	ΔV_0	ΔZPVE	ΔE_0	$ \bar{\nu}_F^\ddagger $ (cm^{-1})
HF	6-31G(<i>d</i>)[89]	76.5	-10.6	65.9	1611.3
	6-311G(<i>d,p</i>)[128]	77.3	-10.6	66.6	1605.1
	6-311G(2 <i>d</i> ,2 <i>p</i>) [168]	72.9	-8.4	64.5	1596.0
	cc-PVTZ [224]	75.4	-9.2	66.2	1575.6
	cc-PVQZ [429]	77.1	-10.0	67.1	1591.8
B3LYP	6-31G(<i>d</i>)	36.4	-9.9	26.5	1033.3
	6-311G(<i>d,p</i>)	36.6	-9.6	26.9	1074.2
	6-311G(2 <i>d</i> ,2 <i>p</i>)	40.3	-10.3	30.0	1092.4
	cc-PVTZ	39.6	-9.1	30.5	1063.3
	cc-PVQZ	41.2	-	-	-
MP2	6-31G(<i>d</i>)	44.8	-10.4	34.4	1125.9
	6-311G(<i>d,p</i>)	43.0	-9.8	33.4	1232.0
	6-311G(2 <i>d</i> ,2 <i>p</i>)	44.4	-10.4	33.7	1246.6
	cc-PVTZ	42.8	-	-	-
	cc-PVQZ	43.1	-	-	-
MP4	6-31G(<i>d</i>)	49.6	-	-	-
	6-311G(<i>d,p</i>)	45.4	-	-	-
CCSD	6-31G(<i>d</i>)	52.6	-	-	-
	6-311G(<i>d,p</i>)	51.6	-	-	-
CCSD(T)	6-31G(<i>d</i>)	48.9	-	-	-
	6-311G(<i>d,p</i>)	46.8	-	-	-

^aNumber of basis functions.

complete basis sets. It should be noted that our lower level [HF/6-311G(*d,p*)] results agree broadly with previous work by Sauer and co-workers,⁹ who report a classical barrier height of 72 kJ mol^{-1} as compared to 77.6 kJ mol^{-1} obtained here, and a harmonic frequency of the reaction coordinate at the transition state of 1520 cm^{-1} , as compared to our result of 1605.1 cm^{-1} . The 3T cluster used in that research does not directly compare to any of our 3T clusters due to different geometrical constraints, and thus will not be discussed in Sec. III B.

The energies and vibrational frequencies depend more strongly on the electronic structure method than they do on variations in the basis set. From our results in Table I, it is seen that a HF treatment of the proton transfer barrier is inadequate. In addition, the assumption that the MP series is monotonically convergent leads to the conclusion that the B3LYP barriers are uniformly too small. This conclusion is supported by the coupled-cluster results, which suggest that even the MP4 barriers are a bit ($1-4 \text{ kJ mol}^{-1}$) too small. Because higher order correlation effects on energy differences are known to converge rapidly with respect to the basis set,^{58,59} it is reasonable to take the difference between the MP2 and MP4 energies with the smaller basis sets as an indication of the probable error, and use that estimate to correct MP2 barriers obtained with larger basis sets. Practical considerations prohibit the use of coupled-cluster methods to study more chemically relevant clusters at this time, and from our results we see that it should not be necessary in order to obtain the desired kcal mol^{-1} accuracy. We use our highest level results to establish error bounds on the MP2/MP4 model chemistry we advocate, demonstrating the effective convergence of ΔV_0 with respect to a degree of corre-

lation at the MP4 level of theory. From Table I we thus expect the MP2 barriers to be a few (<5) kJ mol^{-1} too small, and that the majority of this error is recovered using the MP4 method in a manageable basis set.

MP2 frequencies with moderate basis sets are known to systematically overestimate experimental harmonic frequencies for small gas phase molecules by approximately 6%.⁶⁰ Additionally, systematic DFT studies on small molecules have suggested that the B3LYP method produces harmonic vibrational frequencies that are often closer to experimental values than are the MP2 frequencies for many types of vibrations.⁶¹ For the 1T cluster, we observe that the MP2 and B3LYP methods give nearly identical frequencies for bound vibrational modes (data not shown), with a RMS difference of 50 cm^{-1} , but also give a difference of up to 170 cm^{-1} for the reaction coordinate mode at the transition state. We find no compelling reason in the literature to trust one of these sets of frequencies more than the other, and as such interpret the difference between the MP2 and B3LYP frequencies as our uncertainty. Therefore, the results from our suggested model chemistry augment the ZPVE corrected MP2 barrier height with MP4 single point energies, yielding a value for ΔE_0 of 36.1 kJ mol^{-1} , with an uncertainty of 10 kJ mol^{-1} , and retain the basis-set-converged MP2 value for $|\bar{\nu}_F^\ddagger|$ of 1246 cm^{-1} with an uncertainty of 200 cm^{-1} . The results in Table I using larger basis sets and more complete inclusion of electron correlation demonstrate the validity of this approach.

B. 3T cluster

All of the qualitative conclusions regarding convergence with respect to basis set and level of theory found above for the 1T cluster are echoed by the symmetry constrained 3T clusters. Increasing the Si–Si distance from 5.8 \AA to 6.0 \AA causes the ZPVE corrected barrier height to increase from $\Delta E_0 = 62.8 \text{ kJ mol}^{-1}$ to $105.9 \text{ kJ mol}^{-1}$, while also causing the barrier to narrow from $|\bar{\nu}_F^\ddagger| = 1533 \text{ cm}^{-1}$ to 1682 cm^{-1} . For brevity, we do not discuss these results further. In what follows, we focus on the asymmetric 3T cluster.

Salient geometrical parameters for the asymmetric 3T cluster, calculated at the MP2/6-311G(*d,p*) level of theory, are shown in Fig. 2. With our more chemically relevant cluster, we are able to make meaningful comparisons with results from structural and spectroscopic investigations of H–Y (Si:Al=2.4)²⁸ and Li–LSX (Si:Al=1.0)⁶² zeolites. Comparing with structural data for H–Y allows an analysis of the O–H bond length, H–Al distance, and average T–O bond lengths and T–O–T angles, while comparing with data for Li–LSX allows an analysis of distinct Si–O and Al–O bond lengths as well as specific Si–O–Al angles. A comparison between experimental measurements of these structural parameters and our highest level computations for both the neutral clusters with covalently bound H^+ counterion, and for the anion precursor with no counterion, is made in Table II. At the level shown, MP2/6-311G(*d,p*), the geometrical parameters are converged with respect to both basis set and level of theory to a precision of 0.03 \AA for distances and 3° for angles, and differ from the B3LYP/6-311G(*d,p*) values

TABLE II. Structural parameters of Brønsted acid site from experiment and theory, \AA or deg.

Atoms	Expt.	3T, Anion ^a	3T, O(1)–H ^a	3T, O(4)–H ^a
O–H	0.83 ^b	–	0.962	0.964
T–O(1)	1.68 ^b	1.648 ^c	1.774 ^c	1.669 ^c
T–O(4)	1.64 ^b	1.638 ^c	1.657 ^c	1.770 ^c
Si–O(1)	1.626 ^d	1.596	1.705	1.635
Si–O(4)	1.583 ^d	1.591	1.629	1.708
Al–O(1)	1.701 ^d	1.777	1.943	1.750
Al–O(4)	1.736 ^d	1.753	1.726	1.922
Al–H	2.38 ^e	–	2.451	2.381
T–O(1)–T	135.6 ^b	132.5	128.9	130.4
T–O(4)–T	144.1 ^b	139.7	135.7	135.0
Si–O(1)–Al	143.8 ^d	132.5	128.9	130.4
Si–O(4)–Al	138.6 ^d	139.7	135.7	135.0

^aThis work, MP2/6-311G(*d,p*).

^bCzjzek *et al.* (Ref. 28) H–Y, averaging over T and O sites.

^cTheoretical average; see the text.

^dPlévert *et al.* (Ref. 62) Li–LSX.

^eStevenson, Ref. 63, Freude *et al.* (Ref. 65) H–Y.

by significantly less than that. Despite these accuracies, we recognize that discrepancies between our calculations and experimental data can arise from several sources, notably our truncation of the cluster at three tetrahedral atoms and our neglect of long range interactions.

The T–O(1) and T–O(4) distances as measured by neutron diffraction in H–Y represent averaged values, and hence should be compared with averages of our distances. Because the composition of the H–Y studied in Ref. 28 is $\text{Na}_3\text{H}_{53}\text{Al}_{56}\text{Si}_{136}\text{O}_{384}$, it is not straightforward to devise an appropriate average of our theoretical distances. If we compare to a hypothetical H–Y (Si:Al=2.4) that has been fully proton exchanged, then a plausible theoretical average is $\text{T–O}(1) = (0.29)\text{Al–O}(1) + (0.71)\text{Si–O}(1)$, and likewise for T–O(4). Our averaged T–O distances agree reasonably well with experiment, reproducing all trends. In addition, the comparison of Si–O and Al–O distances and Si–O–Al bond angles with data from Li–LSX gives generally excellent agreement. The small geometric differences between Li–LSX⁶² and our protonated 3T cluster probably arise from the difference between charge compensation by hydrogen and lithium, as well as the fact that our 3T cluster originates from the H–Y crystal structure instead of the Li–LSX structure. In addition, protonation induces a lengthening of the appropriate Al–O bond, towards heterolytically breaking the Al–OH bond as originally proposed.⁶³ The Al–H distances, measured by ^1H NMR⁶⁴ and by combinations of ^1H , ^{27}Al and ^{29}Si NMR,⁶⁵ are in perfect agreement with our results when O(4) is protonated, but disagree with our results by 0.06 \AA when O(1) is protonated. This is not particularly troublesome because, although the experimental result of 2.38 \AA is well established, it is again a value averaged over all occupied protonation sites.

As an aside, the conventional wisdom that the Si–OH–Al moiety is nearly planar,⁶⁶ even when the T–O–T angle is far larger than the standard sp^2 hybridization bond angle of 120° , is consistent with our results. Indeed, we find that the OH bond leaves the plane of the Si–O–Al group at an angle of only 0.04° when O(1) is protonated, and at an

TABLE III. Summary of electronic structure results for 3T cluster. Energies in kJ mol^{-1} .

Basis set [NBF ^a]	Level of theory	ΔV_0	ΔZPVE	ΔE_0	$ \bar{\nu}_F^\ddagger $ (cm^{-1})
6-31G(d)[135]	HF	144.5	-14.2	130.3	2009.7
	BLYP	67.7	-13.6	54.1	1345.7
	B3LYP	85.0	-13.7	71.3	1512.1
	MP2	92.0	-13.6	78.4	1570.2
	MP4 ^b	93.1	-	79.5	-
	CCSD ^b	101.0	-	87.4	-
	CCSD(T) ^b	94.9	-	81.3	-
6-311G(d,p)[204]	HF	150.2	-14.7	135.5	2004.7
	BLYP	72.8	-13.6	59.2	1374.5
	B3LYP	90.2	-13.9	76.3	1528.1
	MP2 ^b	99.1	-	85.5	-
	MP4 ^b	99.7	-	86.1	-

^aNumber of basis functions.^bUsing MP2/6-31G(d) frequencies.

angle of 3.8° when O(4) is protonated. This conclusion may change when interactions with the remainder of the zeolite lattice are included.

In addition to the structural data, the O–H vibrational frequency is a key parameter that is known experimentally. Consensus in the literature places the O–H stretch of silanols on the external surface of zeolite crystals at 3750 cm^{-1} , the O–H stretch that points into the supercage at 3650 cm^{-1} , and the O–H stretch that points into the sodalite cage at 3550 cm^{-1} .²⁸ The intracrystalline hydroxyls are influenced by nearby oxygens as well as long range forces, both of which may serve to soften the O–H bond. Because our cluster models ignore these effects, we expect our calculated O–H frequencies to overestimate the experimental ones, being more characteristic of terminal silanol groups. At the MP2/6-31G(d) level of theory, the O(1)–H stretch is 3777 cm^{-1} and the O(4)–H stretch is 3764 cm^{-1} . At the B3LYP/6-31G(d) and B3LYP/6-311G(d,p) levels of theory, the values of the O(1)–H stretching frequency are 3753 cm^{-1} and 3836 cm^{-1} , respectively; while the values of the O(4)–H stretching frequency are 3746 cm^{-1} and 3809 cm^{-1} , respectively.

For estimating fundamental frequencies from MP2/6-31G(d) and B3LYP/6-31G(d) calculations, scaling factors have been developed by systematic studies of smaller, gas phase molecules. These are as follows: $\lambda[\text{MP2/6-31G(d)}]^{60} = 0.9427$; $\lambda[\text{B3LYP/6-31G(d)}]^{61} = 0.920$. Using these, the scaled frequencies are as follows: MP2/6-31G(d) O(1)–H, 3561 cm^{-1} ; O(4)–H, 3548 cm^{-1} ; B3LYP/6-31G(d) O(1)–H, 3452 cm^{-1} ; O(4)–H, 3446 cm^{-1} . These are all substantially lower than experimental values, calling into doubt the general applicability of these scaling factors in computational materials science.

Having established a reasonable cluster model of H–Y, albeit one without long range forces,¹⁷ we now discuss the energetics of proton transfer in the asymmetric cluster. Table III presents the asymmetric proton transfer transition state parameters for two basis sets and several levels of theory. The MP2 barrier heights in Table III are more than 5 kJ mol^{-1} larger than the B3LYP values, and the MP4 ad-

justment to the MP2 values extends this difference by less than 1.1 kJ mol^{-1} . The coupled cluster results verify our previous conclusion that the MP4 level of theory is nearly converged with respect to the degree of correlation, being within 1.8 kJ mol^{-1} of the CCSD(T) result. Thus, if we seek sub-kcal mol^{-1} accuracy in evaluating barrier heights for proton transfer reactions in zeolites, an explicitly correlated molecular orbital based method such as MP2 is necessary for calculating electronic energies, and the error in the MP2 results is partially recovered using the MP4 method in a smaller basis set. The same requirement is not present for harmonic vibrational frequencies, used to calculate both ZPVE corrections to barrier heights as well as partition functions and barrier curvatures as inputs to rate calculations. The B3LYP/6-31G(d) and MP2/6-31G(d) levels of theory give almost identical vibrational signatures. The difference in ZPVE as calculated by the two methods for any of the stationary points is less than 1.5 kJ mol^{-1} and the values of $|\bar{\nu}_F^\ddagger|$ agree to within 60 cm^{-1} . In addition, the B3LYP/6-31G(d) values of $|\bar{\nu}_F^\ddagger|$ and the ZPVE for each stationary point differ from the B3LYP/6-311G(d,p) values by only 15 cm^{-1} and $0.2\text{--}0.6 \text{ kJ mol}^{-1}$, respectively, suggesting that results in the smaller basis set may be approaching convergence for the 3T cluster. Thus, certain DFT methods such as B3LYP, but not BLYP, may be acceptable for calculating sufficiently accurate vibrational frequencies for these zeolite cluster models.

Our final results, which will be used in the following paper to calculate quantum mechanical proton transfer rates, give a ZPVE corrected classical barrier height of $86.1 \pm 10 \text{ kJ mol}^{-1}$ for the O(1)→O(4) reaction, and $83.6 \pm 10 \text{ kJ mol}^{-1}$ for O(4)→O(1) in H–Y zeolite. The curvature of the barrier is found to be $|\bar{\nu}_F^\ddagger| = 1570 \pm 200 \text{ cm}^{-1}$. By detailed balance, the barrier heights suggest that the proton affinity at O(1) is only 2.5 kJ mol^{-1} greater than that at O(4). This result is inconsistent with powder neutron diffraction (PND) data,²⁸ which find minimal proton binding at O(4). This discrepancy most likely arises from our neglect of long range forces. Sauer *et al.*¹⁷ have reported an embedded cluster calculation on this O(1)→O(4) proton jump, finding that the non-ZPVE-corrected proton affinity at O(1) is $14\text{--}22 \text{ kJ mol}^{-1}$ higher than that at O(4), in much better agreement with PND data. We can use these embedded cluster results to estimate the effect of long range interactions on ZPVE corrected barriers at the MP4 level of theory, with vibrational frequencies calculated using MP2. Doing this gives $\Delta E_0^{\text{Embed}}(\text{MP4}) \cong \Delta V_0^{\text{Embed}}(\text{B3LYP}) + [\Delta E_0^{3\text{T}}(\text{MP4}) - \Delta E_0^{3\text{T}}(\text{B3LYP})] + \Delta \text{ZPVE}^{3\text{T}}(\text{MP2}) = 100.9 + (86.1 - 76.3) - 13.6 \text{ kJ mol}^{-1} = 97.1 \text{ kJ mol}^{-1}$.

These calculated barriers are significantly larger than the 61 kJ mol^{-1} measured by Sarv *et al.*⁵ for proton transfer in H–Y by variable temperature MAS-NMR. We believe that the source of this discrepancy arises primarily from the interpretation of experimental data. Indeed, the rate calculations presented in the following paper suggest that quantum tunneling is the dominant mechanism for proton transfer in H–Y up to and slightly above room temperature, where many of the NMR experiments were performed. Assuming an Arrhenius temperature dependence for proton transfer rates in the tunneling regime will consequently underesti-

mate the true ZPVE corrected barrier. As such, we find it quite plausible that our calculated activation energies are well above experimental values.

C. Recommendations

The above findings lead to specific recommendations for accurately performing converged cluster calculations of the parameters necessary for the rate theory explained in Paper II. Geometric parameters from either B3LYP or MP2, using a basis set that includes a triple- ζ description of the bonding orbitals and polarization functions on all atoms, are accurate to an acceptable degree, especially when terminal atoms are frozen in space to represent the covalent footprint of the bulk zeolite. Harmonic vibrational frequencies evaluated at either level of theory are converged with the basis set above, although the computational efficiency of DFT advocates strongly for its use. For obtaining accurate classical barrier heights, i.e. converged to within 10 kJ mol^{-1} , we find it necessary to use a correlated molecular orbital based approach at least as accurate as MP2, and possibly as accurate (and expensive) as MP4. Fortunately, the difference between MP2 and MP4 barrier heights is found to be small and roughly constant with respect to the basis set, essentially eliminating the need to calculate MP4 energies in large basis sets. Our coupled-cluster results demonstrate that this procedure recovers almost all of the correlation energy contribution to the barrier heights of interest, well within the bounds of "chemical accuracy," approximately 1 kcal mol^{-1} .

IV. CONCLUDING REMARKS

We have applied electronic structure methods to the calculation of transition state parameters for the $\text{O}(1) \leftrightarrow \text{O}(4)$ proton transfer in H-Y zeolite. As shown in the following paper, these parameters are the zero point vibrational energy (ZPVE) corrected classical barrier, ΔE_0 , and the curvature of the barrier at the transition state, $|\bar{\nu}_F^\ddagger|$. By systematically improving basis set expansions and utilizing various correlated levels of theory, we arrive at a set of recommendations for calculating ΔE_0 and $|\bar{\nu}_F^\ddagger|$ accurately and efficiently. We find that basis sets lacking polarization functions on hydrogen atoms consistently fail to produce accurate classical barrier heights regardless of the theoretical method. DFT calculations using the B3LYP functional and basis sets of triple- ζ quality in the valence space, and including polarization functions on all atoms, provide the least computationally expensive treatment yielding substantially converged structural features and harmonic vibrational frequencies. For obtaining classical barrier heights, we find it necessary to use a more traditional, molecular orbital based correlation method. Augmenting barrier heights calculated using an MP2 wave function in a large basis set with MP4 energetics, obtained in a more limited basis set, completes the model chemistry we recommend.

For the proton transfer examined in H-Y zeolite we obtain a forward, $\text{O}(1) \rightarrow \text{O}(4)$ barrier height of 86.1 kJ mol^{-1} , and a reverse, $\text{O}(4) \rightarrow \text{O}(1)$ barrier height of 83.6 kJ mol^{-1} . Estimating the effects of long range interactions from the embedded cluster calculations of Sauer *et al.*¹⁷ gives a final

barrier height of 97.1 kJ mol^{-1} . We find the curvature of the barrier at the transition state to be 1570 cm^{-1} . These calculated barriers are significantly larger than those in the experimental literature.³⁻⁵ We rationalize this discrepancy by noting that experimental analyses are likely to underestimate barriers by assuming an Arrhenius temperature dependence when quantum tunneling is important. In the future, experimental proton transfer rates on a wider range and finer mesh of temperatures, as well as more accurate theoretical calculations, will be required before the importance of proton tunneling in zeolites at ambient conditions is firmly established.

We hope that the findings outlined here will guide future investigations of reactivity at zeolite acid sites. Indeed, we plan to carry out electronic structure calculations on larger cluster models of H-Y, using the recommendations outlined above, to determine how cluster truncation modifies the electronic and vibrational characteristics of proton transfer. We also plan to carry out such calculations on periodic models, to verify the importance of long range forces.

Armed with the harmonic transition state parameters calculated herein, we now turn our attention to the calculation of quantum proton transfer rates. Although previous harmonic quantum rate theories have exhibited instabilities when applied at very low temperatures, in the following paper we develop a novel harmonic semiclassical transition state theory that is easy to parametrize and evaluate, and is stable to arbitrarily low temperatures. Based on this quantum rate theory, we find that tunneling is the dominant mechanism for proton transfer in H-Y up to approximately 370 K.

ACKNOWLEDGMENTS

This work was supported by the National Science Foundation (CHE-9616019 and CTS-9734153), a Sloan Foundation Research Fellowship (BR-3844), and a Camille Dreyfus Teacher-Scholar Award (TC-99-041). The authors gratefully acknowledge computing time on an IBM SP2, supported by Professor. C. Weems of the Computer Science Department, and by Professor F. Byron, Vice Chancellor of Research.

¹J. Weitkamp, in *Catalysis and Adsorption by Zeolites*, edited by G. Olthmann, J. C. Vedrine, and P. A. Jacobs (Elsevier, Amsterdam, 1991), p. 21.

²A. Corma, *Chem. Rev.* **95**, 559 (1995), and references therein.

³T. Baba, N. Komatsu, Y. Ono, and H. Sugisawa, *J. Phys. Chem. B* **102**, 804 (1998).

⁴T. Baba, N. Komatsu, Y. Ono, H. Sugisawa, and T. Takahashi, *Micro. Meso. Mat.* **22**, 203 (1998).

⁵P. Sarv, T. Tuherm, E. Lippmaa, K. Keskinen, and A. Root, *J. Phys. Chem.* **99**, 13763 (1995).

⁶J. Sauer, *Chem. Rev.* **98**, 199 (1989), and references therein.

⁷R. A. van Santen and G. J. Kramer, *Chem. Rev.* **95**, 637 (1995), and references therein.

⁸M. J. Rice, A. K. Chakraborty, and A. T. Bell, *J. Phys. Chem. A* **102**, 7498 (1998).

⁹J. Sauer, C. M. Kolmel, J.-R. Hill, and R. Ahlrichs, *Chem. Phys. Lett.* **164**, 193 (1989).

¹⁰G. J. Kramer and R. A. van Santen, *J. Am. Chem. Soc.* **117**, 1766 (1995).

¹¹M. J. Murphy, G. A. Voth, and A. L. R. Bug, *J. Phys. Chem. B* **101**, 491 (1997).

¹²T. N. Truong, *J. Phys. Chem. B* **101**, 2750 (1997).

- ¹³P. E. Sinclair and C. R. A. Catlow, *J. Phys. Chem. B* **101**, 295 (1997).
- ¹⁴A. H. de Vries, P. Sherwood, S. J. Collins, A. M. Rigby, M. Rigutto, and G. J. Kramer, *J. Phys. Chem. B* **103**, 6133 (1999).
- ¹⁵J. B. Nicholas, R. E. Winans, R. J. Harrison, L. E. Iton, L. A. Curtiss, and A. J. Hopfinger, *J. Phys. Chem.* **96**, 10247 (1992).
- ¹⁶E. Kassab, J. Fouquet, M. Allavena, and E. M. Evleth, *J. Chem. Phys.* **97**, 9034 (1993).
- ¹⁷J. Sauer, M. Sierka, and F. Haase, in *Transition State Modeling for Catalysis*, No. 721 in ACS Symposium Series, edited by D. G. Truhlar and K. Morokuma (ACS, Washington, 1999), Chap. 28, pp. 358–367.
- ¹⁸C. C. J. Roothaan, *Rev. Mod. Phys.* **23**, 69 (1951).
- ¹⁹A. Szabo and N. S. Ostlund, *Modern Quantum Chemistry: Introduction to Advanced Electronic Structure Theory* (McGraw-Hill, New York, 1989).
- ²⁰A. D. Becke, *Phys. Rev. A* **38**, 3098 (1988).
- ²¹C. Lee, W. Yang, and R. G. Parr, *Phys. Rev. B* **37**, 785 (1988).
- ²²A. D. Becke, *J. Chem. Phys.* **98**, 5648 (1993).
- ²³C. Møller and M. S. Plesset, *Phys. Rev.* **46**, 618 (1934).
- ²⁴R. Krishnan and J. A. Pople, *Int. J. Quantum Chem.* **14**, 91 (1978).
- ²⁵R. Krishnan, M. J. Frisch, and J. A. Pople, *J. Chem. Phys.* **72**, 4244 (1980).
- ²⁶J. Sauer, *J. Phys. Chem.* **91**, 2315 (1987).
- ²⁷The Si–O(1)–Al–O(4)–Si distance in H–Y is reported in Ref. 28 to be 5.94 Å. We choose 5.8 Å and 6.0 Å to bracket the experimentally determined distance.
- ²⁸M. Czjzek, H. Jobic, A. N. Fitch, and T. Vogt, *J. Phys. Chem.* **96**, 1535 (1992).
- ²⁹G. Herzberg, *Molecular Spectra and Molecular Structure* (Krieger, Malabar, FL, 1991), Vol. 2.
- ³⁰H. B. Schlegel, *J. Comput. Chem.* **3**, 214 (1982).
- ³¹R. Ditchfield, W. J. Hehre, and J. A. Pople, *J. Chem. Phys.* **54**, 724 (1971).
- ³²W. J. Hehre, R. Ditchfield, and J. A. Pople, *J. Chem. Phys.* **56**, 2257 (1972).
- ³³P. C. Hariharan and J. A. Pople, *Theor. Chim. Acta* **28**, 213 (1980).
- ³⁴P. C. Hariharan and J. A. Pople, *Mol. Phys.* **27**, 209 (1974).
- ³⁵M. S. Gordon, *Chem. Phys. Lett.* **76**, 163 (1980).
- ³⁶A. D. McLean and G. S. Chandler, *J. Chem. Phys.* **72**, 5639 (1980).
- ³⁷R. Krishnan, J. S. Binkley, R. Seeger, and J. A. Pople, *J. Chem. Phys.* **72**, 650 (1980).
- ³⁸R. C. Binning, Jr. and L. A. Curtiss, *J. Comput. Chem.* **11**, 1206 (1990).
- ³⁹T. H. Dunning, *J. Chem. Phys.* **90**, 1007 (1989).
- ⁴⁰D. E. Woon and T. H. Dunning, Jr., *J. Chem. Phys.* **98**, 1358 (1993).
- ⁴¹R. A. Kendall, T. H. Dunning, Jr., and R. J. Harrison, *J. Chem. Phys.* **96**, 6796 (1992).
- ⁴²K. A. Peterson, D. E. Woon, and T. H. Dunning, Jr., *J. Chem. Phys.* **100**, 7410 (1994).
- ⁴³A. Wilson, T. van Mourik, and T. H. Dunning, Jr., *J. Mol. Struct.: THEOCHEM* **388**, 339 (1997).
- ⁴⁴M. J. Frisch *et al.*, GAUSSIAN98, Revision A.3 (Gaussian, Inc., Pittsburgh, PA, 1998).
- ⁴⁵G. D. Purvis and R. J. Bartlett, *J. Chem. Phys.* **76**, 1910 (1982).
- ⁴⁶G. E. Scuseria, C. L. Janssen, and H. F. Schaefer III, *J. Chem. Phys.* **89**, 7382 (1988).
- ⁴⁷K. Raghavachari, G. W. Trucks, J. A. Pople, and M. Head-Gordon, *Chem. Phys. Lett.* **157**, 479 (1989).
- ⁴⁸G. E. Scuseria and T. J. Lee, *J. Chem. Phys.* **93**, 5851 (1990).
- ⁴⁹A. D. Becke, *J. Chem. Phys.* **98**, 1372 (1993).
- ⁵⁰GAUSSIAN98 User's Reference, 2nd ed. (Gaussian, Inc., Carnegie Office Park, Bldg. 6, Pittsburgh, PA 15106, 1999).
- ⁵¹J. A. Pople, R. Krishnan, H. B. Schlegel, and J. S. Binkley, *Int. J. Quantum Chem., Symp.* **13**, 225 (1979).
- ⁵²N. C. Handy and H. F. Schaefer III, *J. Chem. Phys.* **81**, 5131 (1984).
- ⁵³M. Head-Gordon and T. Head-Gordon, *Chem. Phys. Lett.* **220**, 122 (1994).
- ⁵⁴B. G. Johnson and M. J. Frisch, *J. Chem. Phys.* **100**, 7429 (1994).
- ⁵⁵P. Jeffrey Hay (private communication).
- ⁵⁶A. Rodriguez, *Vib. Spectrosc.* **9**, 225 (1995).
- ⁵⁷C. L. Janssen, *et al.*, PSI 2.0.8 (PSITECH, Inc., Watkinsville, GA, 1995).
- ⁵⁸A. L. L. East and W. D. Allen, *J. Chem. Phys.* **99**, 4638 (1993).
- ⁵⁹N. L. Allinger, J. T. Fermann, W. D. Allen, and H. F. Schaefer III, *J. Chem. Phys.* **106**, 5143 (1997).
- ⁶⁰A. P. Scott and L. Radom, *J. Phys. Chem.* **100**, 16502 (1996).
- ⁶¹G. Rauhut and P. Pulay, *J. Phys. Chem.* **99**, 3093 (1995).
- ⁶²J. Plévert, F. D. Renzo, F. Fajula, and G. Chiavi, *J. Phys. Chem. B* **101**, 10340 (1997).
- ⁶³J. B. Uytterhoeven, L. G. Christner, and W. K. Hall, *J. Phys. Chem.* **69**, 2117 (1965).
- ⁶⁴R. L. Stevenson, *J. Catal.* **21**, 113 (1971).
- ⁶⁵D. Freude, J. Klinowski, and H. Hamdan, *Chem. Phys. Lett.* **149**, 355 (1988).
- ⁶⁶Z. Jiráček, S. Vratilav, and V. Bosáček, *J. Phys. Chem. Solids* **41**, 1089 (1980).